Seasonal and Spatial Assessment of Urban Heat Island and Land Surface Temperature in Nagpur Using Landsat Remote Sensing

Authors:

Harsh K. Shinde[1,*], Dr. Sanjay V. Balamwar[1], Sanskar Shete[1]

[1]Digital Image Processing Lab, Maharashtra Remote Sensing Applications Centre,
VNIT Campus, Nagpur 440011, India

This manuscript is a non-peer reviewed preprint submitted to EarthArXiv. It was submitted to the *International Journal of Engineering and Geosciences* for peer review on 05/12/2025.

Corresponding author: Harsh K. Shinde (harshinde.hks@gmail.com)

SEASONAL AND SPATIAL ASSESSMENT OF URBAN HEAT ISLAND AND LAND SURFACE TEMPERATURE IN NAGPUR USING LANDSAT REMOTE SENSING

Harsh K. Shinde,* **Dr. Sanjay V. Balamwar**, **Sanskar Shete**
Digital Image Processing Lab
Maharashtra Remote Sensing Applications Centre
VNIT Campus, Nagpur, India
harshinde.hks@gmail.com, sv.balamwar@mrsac.gov.in, sanskarrshete.rs@gmail.com

https://github.com/HarshShinde0/MRSAC

ABSTRACT

Urban Heat Island (UHI) intensity and Land Surface Temperature (LST) variations are critical indicators of urban environmental change in rapidly growing cities. This study examines spatial and temporal UHI and LST patterns in Nagpur using Landsat 8 and 9 thermal imagery for January and May of 2023 and 2024, capturing seasonal and inter-annual variations. Supervised classification was applied to map Land Use Land Cover (LULC) classes in 2024, and LST was derived using standard radiometric conversion workflows. Comparative analysis between years revealed LST mean variations ranging from 27.4°C to 29.9°C across seasons, with UHI intensities spanning from -19.9°C to 18.3°C. Strong correlations between LULC types and surface temperatures underscore the influence of built-up areas and vegetation on urban thermal patterns. This integrated remote sensing assessment provides actionable insights for urban thermal management and supports climate-responsive urban planning in mid-sized Indian cities.

Keywords Remote sensing · Land surface temperature · Urban heat island intensity · Earth Observation

1. Introduction

Urban Heat Island (UHI) and Land Surface Temperature (LST) have become essential indicators for understanding the impacts of rapid urbanization on local climate systems [1, 2]. As cities expand, changes in land cover, increased built-up surfaces, and reduced vegetation intensify surface heating, leading to higher urban temperatures compared to surrounding rural areas [3, 4]. LST derived from satellite observations offers a reliable means to assess these thermal variations and provides critical insights for climate adaptation and urban planning [5, 6].

Nagpur, a rapidly developing city in Maharashtra, presents an important setting for examining these dynamics due to its growing urban footprint and exposure to increasing heat stress. Although several studies have explored UHI patterns in large Indian metros, limited attention has been given to mid-sized cities like Nagpur, where thermal behavior is shaped by rapid development and semi-arid climatic conditions [7].

This study investigates the spatial and temporal variation of UHI and LST in Nagpur by comparing two consecutive years, 2023 and 2024, using thermal data from Landsat 8 and Landsat 9 [8]. To capture seasonal contrasts, satellite imagery from January and May representing cooler and hotter periods was analyzed for both years. This temporal analysis across two years and two seasons enables understanding of how surface temperatures vary seasonally and inter-annually.

*Corresponding author.
E-mail address: harshinde.hks@gmail.com (H. Shinde).

Land Use Land Cover (LULC) information for 2024 supports the interpretation of surface temperature patterns, reflecting the influence of built-up areas, vegetation, and other land surface types [9, 10]. Together, these components provide a comprehensive perspective on recent thermal behavior in Nagpur and contribute to the growing need for localized urban climate assessments in Indian cities.

2. Methodology

2.1. Study area

Nagpur city is located in the state of Maharashtra, India, and lies geographically between 20°30'N to 21°45'N latitude and 78°15'E to 79°45'E longitude. Positioned near the geographical centre of India, Nagpur serves as a major urban hub in central India and is considered one of the rapidly growing cities of the region. The city has a population of approximately 2.405 million, and its continuous urban expansion is significantly reshaping the local environment.

Nagpur experiences a predominantly hot and dry climate, with dry conditions prevailing for most of the year. The region shows strong seasonal variability, with temperatures rising to 37°C–45°C during April–May and dropping to around 10°C during December–January. Annual precipitation ranges from 1000 mm to 1800 mm, mainly occurring during the monsoon season. Extreme summer temperatures reaching up to 44°C and frequent heat-wave events contribute to substantial thermal discomfort for residents.

The city's rapid urban growth, increasing built-up areas, and reduction in vegetation have amplified concerns related to surface heating. These changes intensify the Urban Heat Island (UHI) effect, making temperature management an important consideration for urban planning [11, 12]. Understanding the spatial distribution of surface temperature and its relationship with land cover is therefore essential for improving thermal comfort and supporting climate-responsive development in Nagpur.

2.2. Data Source

This study employed multispectral satellite imagery from Landsat 8 and Landsat 9, accessed through the Microsoft Planetary Computer. These sensors were selected for their consistent temporal coverage and for providing Thermal Infrared (TIRS) bands essential for accurate Land Surface Temperature (LST) estimation [13, 14]. To capture seasonal and inter-annual variations in Nagpur's thermal environment, imagery from January 2023 and May 2023 was used to represent the cold and hot seasons of 2023, while January 2024 and May 2024 were used to represent the corresponding seasons for 2024.

All selected images had low cloud cover, ensuring high-quality datasets with minimal atmospheric interference. As Nagpur lies across Landsat Path/Row 144/045 and 144/046, imagery from both tiles was acquired to ensure complete spatial coverage of the study area. After acquisition, the scenes were clipped to the municipal boundary to isolate the region of interest.

The Landsat series was chosen primarily for its thermal imaging capability, which allows for precise extraction of LST and facilitates assessment of Urban Heat Island (UHI) characteristics [15]. The thermal bands (Band 10 and Band 11) from these satellites were processed to derive Land Surface Temperature using standard radiative transfer equation methods. Standard preprocessing steps such as radiometric correction, extraction of thermal bands, and spatial subsetting were carried out to prepare the imagery for subsequent analysis.

2.3. Data Preprocessing and Preparation

All Landsat 8 and Landsat 9 scenes were preprocessed in Python prior to analysis. A custom acquisition pipeline was implemented to query the Microsoft Planetary Computer for Landsat Collection 2 Level-2 scenes within the four study periods (January 2023, May 2023, January 2024, May 2024). For each period, only scenes with less than 10% cloud cover were selected, and pairs of scenes corresponding to Path/Row 144/045 and 144/046 acquired on the same date were identified to ensure complete coverage of the Nagpur urban region.

For every time period, the Level-2 products for each row were first organized into separate folders and processed independently. Spectral bands B1–B10 were merged into a single multi-band GeoTIFF per row, after which the two row-wise composites were mosaicked to produce one continuous image for each period, fully covering the study area. This workflow ensured consistent spatial resolution and radiometric properties across the entire urban extent.

The mosaicked images were then clipped to the Nagpur municipal boundary using a vector mask derived from the NGP boundary shapefile. This step restricted all subsequent analyses strictly to the urban region and excluded surrounding

rural or non-urban areas. Scenes with higher cloud contamination were discarded during the selection stage, so only low cloud-cover, analysis-ready mosaics were retained.

Figure 1: Location of the study region.

2.4. Land Use Land Cover (LULC) Classification

Land Use Land Cover (LULC) classification was conducted for the year 2024 using a supervised classification approach in ArcGIS Pro. The analysis utilized the Nagpur mosaic generated from the merged multispectral bands of Landsat 9, ensuring complete coverage of the urban extent. Based on the predominant landscape characteristics of the region, five land cover classes were defined: Water, Developed (Built-up), Barren land, Forest, and Planted/Cultivated areas.

Training samples representing each land cover class were created through detailed visual interpretation of the multi-spectral imagery, supported by local environmental knowledge. The Support Vector Machine (SVM) classifier was employed due to its strong capability in handling high-dimensional spectral data and its effectiveness in separating classes with overlapping spectral signatures [16–18]. The trained classifier was used to generate the final LULC map for 2024.

Accuracy assessment was performed using high-resolution reference imagery and contextual field knowledge to verify the reliability of class assignments. As the study period (2023–2024) exhibited minimal land cover change, the 2024 LULC map was used as a representative reference for interpreting surface temperature variations and urban thermal behavior across both years.

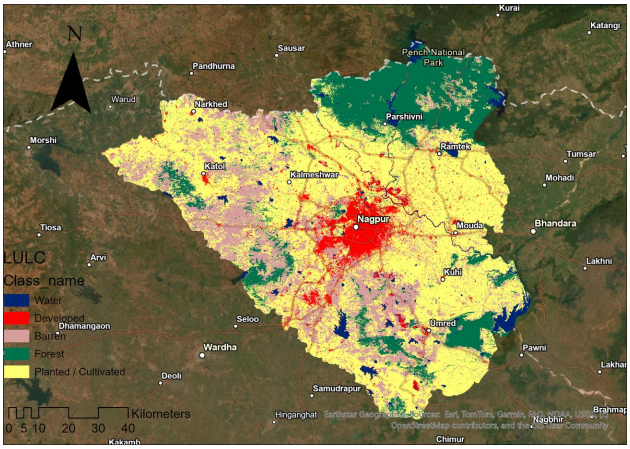

Figure 2: Land Use Land Cover classification for Nagpur (2024).

2.5. Extracting Land Surface Temperature and Urban Heat Island

Land Surface Temperature (LST) was derived from the thermal infrared bands of Landsat 8 and Landsat 9 using a standard radiometric conversion workflow [8]. The extraction process consisted of converting digital number (DN) values into top-of-atmosphere (TOA) radiance, transforming radiance to at-sensor brightness temperature, and applying emissivity correction to obtain accurate surface temperature estimates. This procedure ensures consistency across sensors and acquisition dates, enabling reliable comparison of thermal conditions between seasons and years. Urban Heat Island (UHI) intensity was subsequently assessed by contrasting pixel-level LST values with a scene-wide background reference temperature, allowing the identification and evaluation of localized thermal anomalies within the Nagpur urban area.

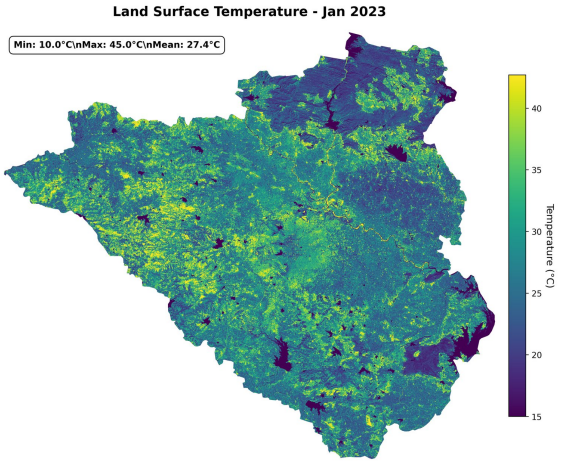

Figure 3: (a) January 2023 LST

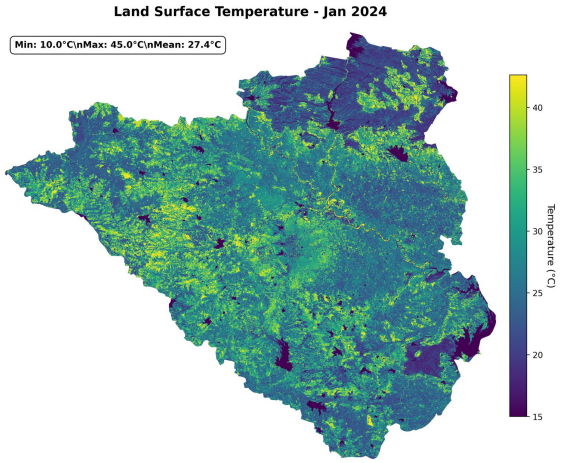

Figure 4: (b) January 2024 LST

Figure 5: Land Surface Temperature comparison for January (2023 vs 2024).

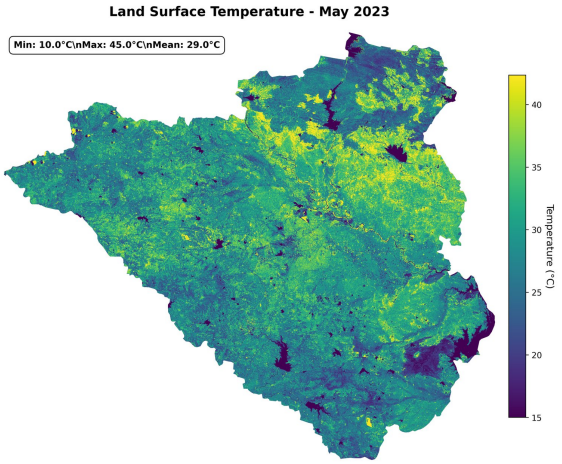

Figure 6: (a) May 2023 LST

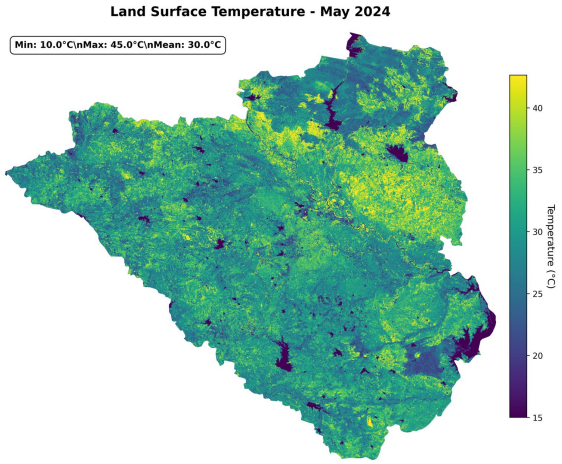

Figure 7: (b) May 2024 LST

Figure 8: Land Surface Temperature comparison for May (2023 vs 2024).

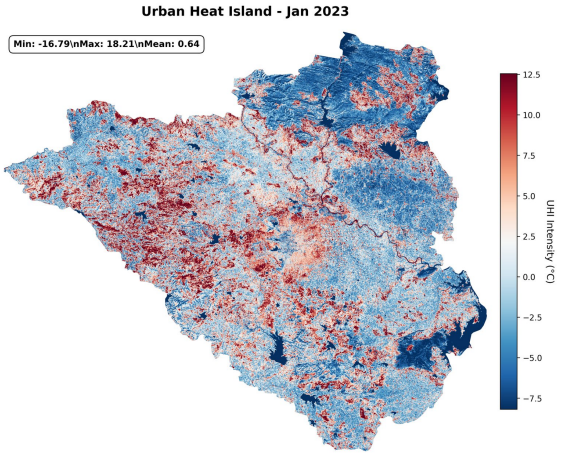

Figure 9: (a) January 2023 UHI

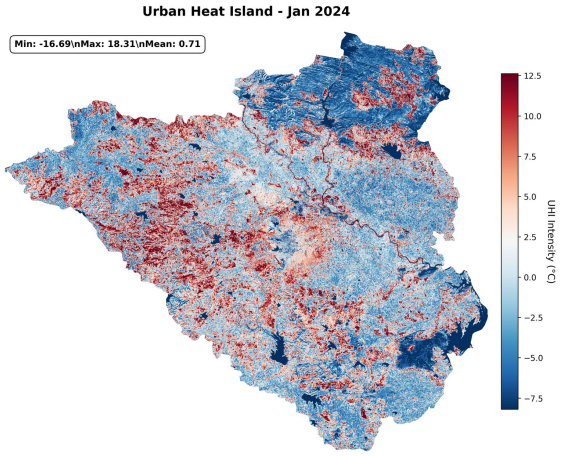

Figure 10: (b) January 2024 UHI

Figure 11: Urban Heat Island comparison for January (2023 vs 2024).

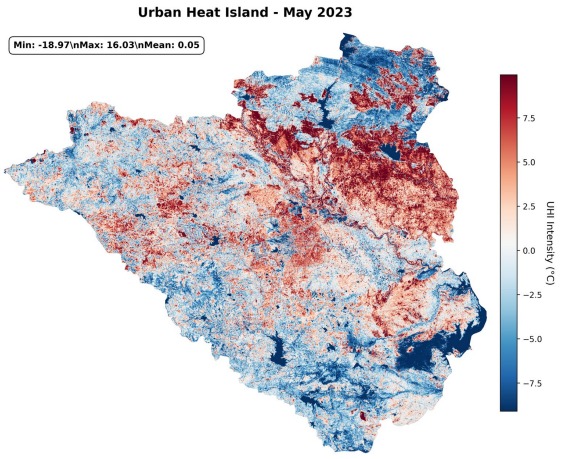

Figure 12: (a) May 2023 UHI

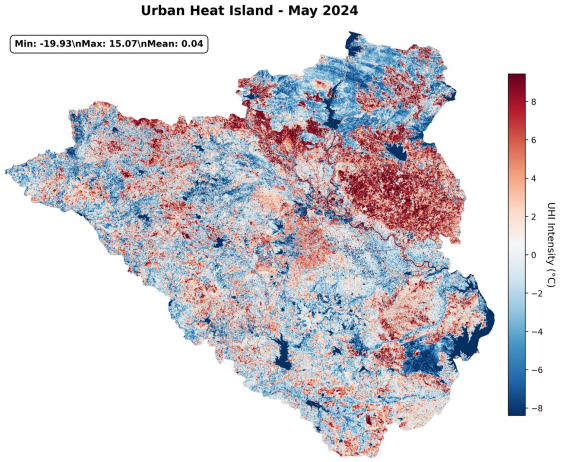

Figure 13: (b) May 2024 UHI

Figure 14: Urban Heat Island comparison for May (2023 vs 2024).

Table 1: Variation of Mean LST for 2023 and 2024

Period	LST Min (°C)	LST Max (°C)	LST Mean (°C)	LST Std (°C)
Jan 2023	10.000	45.000	27.432	6.584
Jan 2024	10.000	45.000	27.395	6.665
May 2023	10.000	45.000	29.016	5.971
May 2024	10.000	45.000	29.964	5.756

Table 2: Variation of Mean UHI Intensity for 2023 and 2024

Period	UHI Min (°C)	UHI Max (°C)	UHI Mean (°C)	UHI Std (°C)
Jan 2023	-16.788	18.212	0.644	4.237
Jan 2024	-16.687	18.313	0.708	4.342
May 2023	-18.967	16.033	0.048	3.156
May 2024	-19.926	15.074	0.038	3.089

(1) Conversion of DN to Radiance

Digital numbers for each thermal pixel were converted to TOA spectral radiance using the Landsat radiometric rescaling coefficients:

$$L_\lambda = M_L \times Q_{\text{cal}} + A_L \tag{1}$$

where

- L_λ = TOA spectral radiance
- M_L = radiance multiplicative scaling factor
- A_L = radiance additive scaling factor
- Q_{cal} = pixel DN of the thermal band

(2) Radiance to Brightness Temperature

Radiance was converted to at-sensor brightness temperature using the thermal calibration constants:

$$T_B = \frac{K_2}{\ln\left(\frac{K_1}{L_\lambda} + 1\right)} \tag{2}$$

where

- T_B = brightness temperature (K)
- K_1, K_2 = thermal calibration constants for the Landsat thermal band

(3) Land Surface Temperature (LST)

Brightness temperature was corrected for surface emissivity to estimate the actual land surface temperature:

$$T_s = \frac{T_B}{1 + \lambda T_B \rho \ln(\varepsilon)} - 273.15 \tag{3}$$

where

- T_s = land surface temperature (°C)
- λ = effective wavelength of the thermal band
- $\rho = \frac{hc}{\sigma}$ (constant derived from Planck's law)
- ε = land surface emissivity

Emissivity values were assigned based on land cover characteristics using standard emissivity reference models.

(4) Urban Heat Island (UHI) Estimation

UHI intensity was quantified using the relative surface temperature method. For each time period, the median LST of non-urban areas was used as a background reference. The UHI intensity at each pixel was computed as:

$$\text{UHI} = T_I - T_A \tag{4}$$

where

- T_I = LST of the urban pixel
- T_A = reference background temperature (median LST of the scene)

This approach highlights localized thermal hotspots and enables seasonal and inter-annual comparison of UHI behavior across Nagpur.

Together, these steps establish a consistent and reliable framework for retrieving surface temperature and assessing heat island intensity across the study area. By standardizing radiometric conversion, brightness temperature calculation, emissivity correction, and UHI estimation, the method enables meaningful comparison of thermal characteristics between seasons and years. The resulting LST and UHI datasets provide a robust foundation for evaluating spatial thermal patterns, identifying persistent hot and cold regions, and examining the influence of urban development on surface heating within Nagpur.

2.6. Derivation of Normalized Difference Vegetation Index (NDVI)

Normalized Difference Vegetation Index (NDVI) was computed to evaluate vegetation distribution and its influence on surface temperature patterns within Nagpur [5]. NDVI is widely used in urban climate studies as an indicator of vegetation density, enabling assessment of the cooling effect provided by green cover and its role in moderating Urban Heat Island formation [19, 20]. For this study, NDVI was derived from the red and near-infrared (NIR) reflectance bands of Landsat 8 and Landsat 9 for all four temporal datasets: January 2023, May 2023, January 2024, and May 2024.

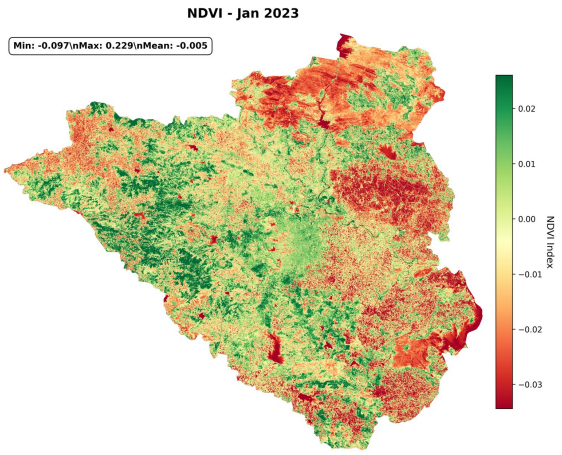

Figure 15: (a) January 2023 NDVI

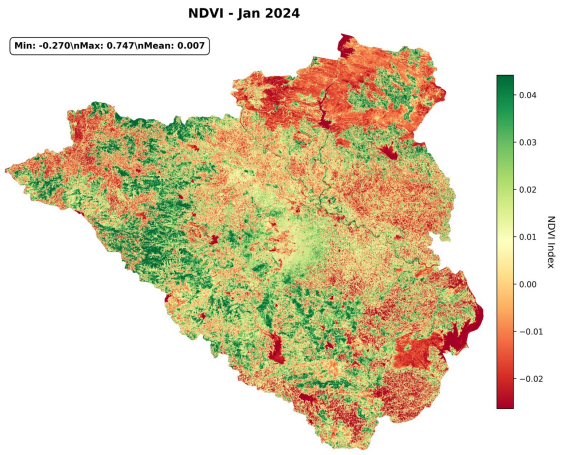

Figure 16: (b) January 2024 NDVI

Figure 17: Normalized Difference Vegetation Index comparison for January (2023 vs 2024).

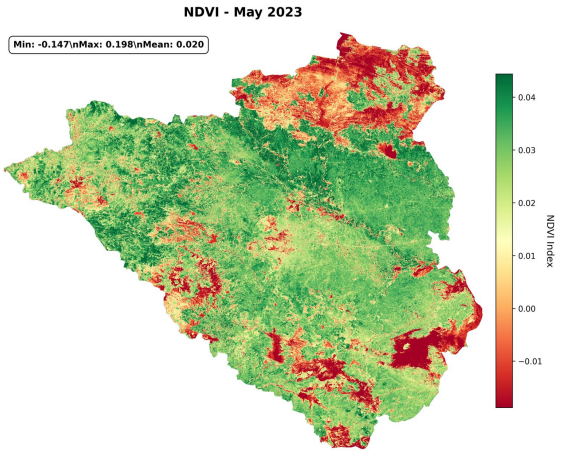

Figure 18: (a) May 2023 NDVI

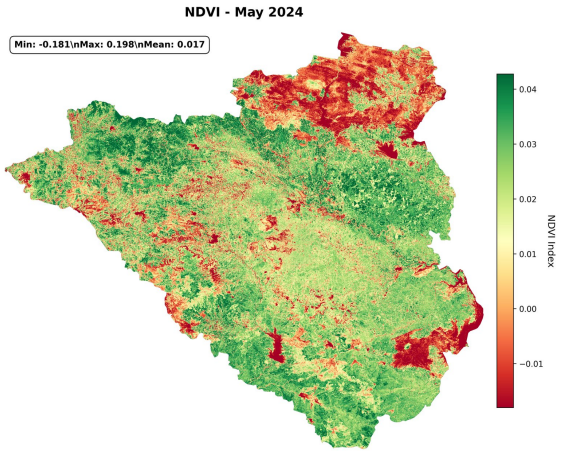

Figure 19: (b) May 2024 NDVI

Figure 20: Normalized Difference Vegetation Index comparison for May (2023 vs 2024).

The index was calculated using the standard formulation:

$$\text{NDVI} = \frac{\text{NIR} - \text{Red}}{\text{NIR} + \text{Red}} \tag{5}$$

where

- NIR = Near-infrared reflectance (Band 5 for Landsat 8/9)
- Red = Red band reflectance (Band 4 for Landsat 8/9)

The NDVI results reveal clear seasonal and inter-annual variability in vegetation cover across Nagpur. Both years show comparatively higher NDVI values in January, reflecting increased vegetation moisture and reduced heat stress during the winter season. Conversely, NDVI values are lower in May due to dry-season conditions and reduced vegetation vigor. Minor changes between 2023 and 2024 suggest stable land cover conditions, consistent with the limited LULC change observed during the study period. These vegetation patterns play an important role in modulating LST, helping to explain spatial differences in cooling and heating across the urban landscape.

3. Results and Discussion

The analysis across the four study periods shows clear seasonal differences in surface temperature across Nagpur [4]. Winter months recorded moderate temperatures, with mean LST values of 27.43 °C in January 2023 and 27.39 °C in January 2024, while summer months showed notably higher values, increasing to 29.02 °C in May 2023 and 29.96 °C in May 2024. These patterns reflect Nagpur's hot, semi-arid climate, where strong pre-monsoon heating raises surface temperatures across the city. The small difference between the two years suggests limited land-cover change during the study period.

Spatial patterns show that higher temperatures consistently occur in the southern and eastern parts of Nagpur, where built-up areas, barren land, and sparse vegetation dominate. Cooler surfaces appear mostly in the northern region, influenced by forested zones, agricultural land, and water bodies [10]. Winter months show slightly greater variation in LST than summer, indicating more diverse surface conditions during cooler periods.

Urban Heat Island (UHI) effects follow a similar seasonal trend [6]. UHI intensity is stronger during winter, with mean values of 0.64 °C in January 2023 and 0.71 °C in January 2024, showing a clearer contrast between urban and surrounding areas. In summer, mean UHI drops to 0.05–0.04 °C, as both urban and rural surfaces heat up rapidly under extreme temperatures. Despite lower seasonal averages, localized hotspots persist throughout the city, especially in dense built-up zones.

Vegetation patterns, indicated by NDVI, help explain these thermal differences [16]. NDVI values remain low across all periods, reflecting limited vegetation cover in the urban landscape. Greener areas particularly in northern Nagpur show noticeably lower temperatures, while built-up and barren zones correspond to high-LST hotspots. NDVI values peak in January 2024 (maximum 0.747), showing seasonal green patches, but decline sharply in May due to heat and moisture stress. Overall, the results show that areas with low vegetation experience higher temperatures, reinforcing the close link between land cover and urban thermal behavior.

4. Conclusion

This study provides a two-year assessment of seasonal and spatial variations in Land Surface Temperature (LST) and Urban Heat Island (UHI) patterns in Nagpur using Landsat 8 and Landsat 9 data. The results show a clear seasonal cycle, with noticeably higher temperatures during summer and more moderate conditions in winter [7, 12]. Differences between 2023 and 2024 are minimal, suggesting that land cover in the city remained largely stable during the study period. Hotspots consistently appear in the southern and eastern parts of Nagpur, where built-up and barren surfaces dominate, while cooler temperatures are found in the greener northern areas [15]. UHI intensity is stronger in winter due to clearer contrasts between urban and rural surfaces, whereas summer shows reduced UHI differences because the entire region heats up uniformly.

These findings highlight the important role of vegetation and land cover in shaping Nagpur's thermal environment [10, 14]. Areas with limited greenery experience higher surface temperatures, while regions with more vegetation maintain cooler conditions. The combined LST, UHI, and NDVI results provide a clear understanding of how urban form influences thermal behavior across the city. This evidence can support climate-responsive planning and guide

targeted interventions such as increasing green cover or protecting vegetated zones to help reduce heat stress and improve environmental comfort for residents [1, 2].

Acknowledgments

We thank the Maharashtra Remote Sensing Applications Centre (MRSAC) for institutional support and computing resources. We are grateful to Dr. Sanjay V. Balamwar, Associate Scientist, for valuable guidance and mentorship during this project.

References

[1] G. Manoli, S. Fatichi, M. Schläpfer, K. Yu, N. Nazarian, E. Bou-Zeid, and A. Rinaldo. Magnitude of urban heat islands largely explained by climate and population. *Nature*, 573(7772):55–60, 2019. doi: 10.1038/s41586-019-1512-9.

[2] E. J. Gago, J. Roldan, R. Pacheco-Torres, and J. Ordóñez. The city and urban heat islands: A review of strategies to mitigate adverse effects. *Renewable and Sustainable Energy Reviews*, 25:749–758, 2013. doi: 10.1016/j.rser.2013.05.057.

[3] A. Buyantuyev and J. Wu. Urban heat islands and landscape heterogeneity: Linking spatiotemporal variations in surface temperatures to land-cover and socioeconomic patterns. *Landscape Ecology*, 25(1):17–33, 2010. doi: 10.1007/s10980-009-9402-4.

[4] R. Amiri, Q. Weng, A. Alimohammadi, and S. K. Alavipanah. Spatial-temporal dynamics of land surface temperature in relation to fractional vegetation cover and land use/cover in the tabriz urban area, iran. *Remote Sensing of Environment*, 113(12):2606–2617, 2009. doi: 10.1016/j.rse.2009.07.021.

[5] F. Yuan and M. E. Bauer. Comparison of impervious surface area and normalized difference vegetation index as indicators of surface urban heat island effects in landsat imagery. *Remote Sensing of Environment*, 106(3): 375–386, 2007. doi: 10.1016/j.rse.2006.09.003.

[6] B. Chun and J.-M. Guldmann. Spatial statistical analysis and simulation of the urban heat island in high-density central cities. *Landscape and Urban Planning*, 125:76–88, 2014. doi: 10.1016/j.landurbplan.2014.01.016.

[7] J. Borbora and A. K. Das. Summertime urban heat island study for guwahati city, india. *Sustainable Cities and Society*, 11:61–66, 2014. doi: 10.1016/j.scs.2013.12.001.

[8] P. Fu and Q. Weng. Consistent land surface temperature data generation from irregularly spaced landsat imagery. *Remote Sensing of Environment*, 184:175–187, 2016. doi: 10.1016/j.rse.2016.06.019.

[9] M. Friedl and D. Sulla-Menashe. Modis collection 6 land cover dynamics (mcd12q1): Algorithm description and product overview. *Remote Sensing of Environment*, 253:112136, 2022. doi: 10.1016/j.rse.2020.112136.

[10] A. Asgarian, B. J. Amiri, and Y. Sakieh. Assessing the effect of green cover spatial patterns on urban land surface temperature using landscape metrics approach. *Urban Ecosystems*, 18(1):209–222, 2015. doi: 10.1007/s11252-014-0387-7.

[11] H. B. C. Feng, X. B. Zhao, F. B. Chen, and L. Wu. Using land use change trajectories to quantify the effects of urbanization on urban heat island. *Advances in Space Research*, 53(3):463–473, 2014. doi: 10.1016/j.asr.2013.11.028.

[12] M. Bokaie, M. K. Zarkesh, P. D. Arasteh, and A. Hosseini. Assessment of urban heat island based on the relationship between land surface temperature and land use/land cover in tehran. *Sustainable Cities and Society*, 23:94–104, 2016. doi: 10.1016/j.scs.2016.03.009.

[13] Z. Li, C. Wang, and A. Smith. Dynamic world: Near real-time global 10 m land use/land cover mapping. *Scientific Data*, 11:1387672, 2024. doi: 10.1038/s41597-022-01307-4.

[14] M. Zwolska and J. Kowalski. Urban growth's implications on land surface temperature. *Scientific Reports*, 14: 58501–58512, 2024. doi: 10.1038/s41598-024-58501-0.

[15] X. L. Chen, H. M. Zhao, P. X. Li, and Z. Y. Yin. Remote sensing image-based analysis of the relationship between urban heat island and land use/cover changes. *Remote Sensing of Environment*, 104(2):133–146, 2006. doi: 10.1016/j.rse.2005.11.016.

[16] C. Deng and C. Wu. Bci: A biophysical composition index for remote sensing of urban environments. *Remote Sensing of Environment*, 127:247–259, 2012. doi: 10.1016/j.rse.2012.09.009.

[17] C. Deng and C. Wu. A spatially adaptive spectral mixture analysis for mapping subpixel urban impervious surface distribution. *Remote Sensing of Environment*, 133:62–70, 2013. doi: 10.1016/j.rse.2013.02.005.

[18] C. Deng and C. Wu. Examining the impacts of urban biophysical compositions on surface urban heat island: A spectral unmixing and thermal mixing approach. *Remote Sensing of Environment*, 131:262–274, 2013. doi: 10.1016/j.rse.2012.12.020.

[19] L. Y. Xu, X. D. Xie, and S. Li. Correlation analysis of the urban heat island effect and the spatial and temporal distribution of atmospheric particulates using tm images in beijing. *Environmental Pollution*, 178:102–114, 2013. doi: 10.1016/j.envpol.2013.03.006.

[20] P. Santosh and K. Ramesh. Mapping global forest change using hansen's dataset in google earth engine. *Environmental Data Science*, 2(2):45–60, 2024. doi: 10.1017/eds.2024.8.